UCY – PHY – 02/03

Gamma radiation measurements and dose rates in commercially-used natural tiling rocks (granites)

Michalis Tzortzis and Haralabos Tsertos*

Department of Physics, University of Cyprus, Nicosia, Cyprus

Stelios Christofides and George Christodoulides

Medical Physics Department, Nicosia General Hospital, Nicosia, Cyprus

Abstract

The gamma radiation in samples of a variety of natural tiling rocks (granites) imported in Cyprus for use in the building industry was measured, employing high-resolution γ–ray spectroscopy. The rock samples were pulverized, sealed in 1 *litre* plastic Marinelli beakers, and measured in the laboratory with a live-time between 10 and 14 *hours* each. From the measured γ–ray spectra, activity concentrations were determined for ^{232}Th (range from 1 to 906 $Bq\ kg^{-1}$), ^{238}U (from 1 to 588 $Bq\ kg^{-1}$) and ^{40}K (from 50 to 1606 $Bq\ kg^{-1}$). Elemental concentrations mean values of (35.2 ± 8.4) *ppm*, (6.2 ± 1.8) *ppm* and (4.0 ± 0.2) % were deduced, for thorium, uranium and potassium, respectively. The total absorbed dose rates in air calculated from the concentrations of the three radionuclides, ^{232}Th and ^{238}U series and ^{40}K, ranged from 7 to 1209 $nGy\ h^{-1}$ for full

* *Corresponding author. E-mail address: tsertos@ucy.ac.cy, Fax: +357-22339060*
Department of Physics, University of Cyprus, P. O. Box 20537, 1678 Nicosia, Cyprus.

utilization of the materials, from 4 to 605 *nGy* h^{-1} for half utilization and from 2 to 302 *nGy* h^{-1} for one quarter utilization. The total effective dose rates per person indoors were determined to be between 0.02 to 2.97 *mSv* y^{-1} for half utilization of the materials.

Keywords: natural radioactivity; activity/elemental concentration; absorbed dose rate; annual effective dose rate; radiation exposure; potassium; thorium; uranium; tiling rocks (granites); activity utilization index.

1. Introduction

Gamma radiation from radionuclides which are characterized by *half-lives* comparable to the age of the earth, such as ^{40}K and the radionuclides from the ^{238}U and ^{232}Th series, and their decay products, represents the main external source of irradiation to the human body. The absorbed dose rate in air from cosmic radiation outdoors at sea level is about 30 *nGy* h^{-1} for the southern hemisphere (UNSCEAR 2000 Report). External exposures outdoors arise from terrestrial radionuclides occurring at trace levels in all ground formations. Therefore, the natural environmental radiation mainly depends on geological and geographical conditions (Florou and Kritidis, 1992). Higher radiation levels are associated with igneous rocks, such as granite, and lower levels with sedimentary rocks. There are exceptions, however, as some shales and phosphate rocks have relatively high content of radionuclides (UNSCEAR 2000 Report).

Granites are the most abundant plutonic rocks of mountain belts and continental shield areas. They occur in great batholiths that may occupy thousands of square kilometres and are usually closely associated with quartz monzonite, granodiorite, diorite, and gabbro. They are extremely durable and scratch resistant; their hardness lends themselves for the stone to be mechanically polished to a high gloss finish. Their variety of colour and unique heat and scratch resistant properties makes them ideal for use as

work-surface or as flooring or external and internal cladding. They mainly consist of coarse grains of quartz, potassium feldspar and sodium feldspar. Other common minerals that granites consist of, include mica and hornblende. Typical granites are chemically composed by 75 % silica, 12 % aluminium, less than 5 % potassium oxide, less than 5 % soda, as well as by lime, iron, magnesia, and titania in smaller quantities. Originally, it was widely believed that granites were formed mainly from magmatic differentiation of basaltic magma, evidence that was considered to indicate a metamorphic origin. However, because of the large quantities of granites that occur in nature, geologists believe now that most of the granites have been formed either by melting, partial melting, or metamorphism of deeply buried shale and sandstone. Granites, therefore, are the result of rapidly injected coalescing sheets of magma, each of which cooled independent of the other sheets. Evidence of intrusion or great mobility indicates an igneous origin that stems from melting of sediments, and consequently granite dykes are clearly igneous (Snelling and Woodmorappe, 1998).

In this paper, the results from gamma radiation measurements in samples of a variety of natural tiling rocks imported in Cyprus and sold under the commercial name of "granites" are presented. These results are of general interest since such rocks are globally used as building and ornamental materials. The measurements have been carried out in the Nuclear Physics Laboratory of the Department of Physics, University of Cyprus, using a high-resolution γ–ray spectroscopic system.

2. Experimental method

2.1 Gamma-ray detection system

A stand-alone high-resolution spectroscopic system is used for the measurement of the energy spectrum of the emitted gamma rays in the energy range between 50 *keV* and

3000 *keV*. The system consists of a high-purity germanium (HPGe) detector (coaxial cylinder of 55 *mm* in diameter and 73 *mm* in length) with an efficiency of 30 %, relative to a 3″×3″ NaI(T*l*) scintillator. During operation the detector is cooled down by liquid nitrogen, and its warm-up sensor is coupled to the high-voltage detector bias supply, which is equipped with a remote shutdown feature. The signal-processing electronics includes a spectroscopy main amplifier which incorporates an efficient pile-up rejector, and a Multi-Channel Buffer (MCB) which is a PC-based plug-in PCI card consisting of an 8k Analogue-to-Digital Converter (ADC). An advanced Multi-Channel Analyser (MCA) emulation software (MAESTRO-32) enables data acquisition, storage, display and online analysis of the acquired gamma spectra.

The detector is surrounded by a graded-Z cylindrical shield consisting of lead, iron, and aluminium with thickness of 5 *cm*, 1 *cm*, and 1 *cm*, respectively, which provides an efficient suppression of the background gamma radiation present at the laboratory site. The energy-dependent detection efficiency has been determined using a calibrated ^{152}Eu gamma reference source (standard Marinelli beaker with 85 *mm* bore diameter), which has an active volume of 1000 *ml* and an average density of 1 $g\,cm^{-3}$. The energy resolution (FWHM) achieved in the measurements is 1.8 *keV* at the 1.33 *MeV* reference transition of ^{60}Co.

2.2 Sample preparation and counting

A total of 28 different kinds of “granites” of those imported in Cyprus have been collected (Table 1). The measured samples were pulverized, sieved through 0.2 *mm* mesh, sealed in standard 1000 *ml* Marinelli beakers, dry-weighed and stored for four weeks before counting in order to allow the in-growth of uranium and thorium decay products and achievement of equilibrium for ^{238}U and ^{232}Th with their respective

progeny (Myrick et al., 1983). However, significant non-equilibrium is uncommon in rocks older than 10^6 *years*, and the ^{232}Th series may be considered in equilibrium in most geological environments (Chiozzi et al., 2002). Each sample was put into the shielded HPGe detector and measured for a live-time between 10 and 14 *hours* (a typical spectrum is shown in Fig. 1). Prior to the samples measurement, the environmental gamma background at the laboratory site has been determined with an empty Marinelli beaker under identical measurement conditions. It has been later subtracted from the measured γ–ray spectra of each sample.

The offline analysis of each measured γ–ray spectrum has been carried out by a dedicated software programme (GammaVision-32), which performs a simultaneous fit to all the statistically significant photopeaks appearing in the spectrum. Menu-driven reports were generated which included the centroid channel, energy, net area counts, background counts, intensity and width of identified and unidentified peaks in the spectrum, as well as peak and average activity in $Bq\ kg^{-1}$ for each detected radionuclide. The results of the reported activity concentrations obtained for each of the measured samples, as well as average activity and standard deviation are summarised in Table 1. It is noted here that no other radionuclide than naturally occurring were detected in the measured samples.

2.3 Calculation of elemental concentrations

Calculations of count rates for each detected photopeak and radiological concentrations (activity per mass unit) of detected radionuclides depend on the establishment of secular equilibrium in the samples. Due to the much smaller lifetime of the daughter radionuclides in the decay series of ^{232}Th and ^{238}U, the ^{232}Th concentration was determined from the average concentrations of ^{212}Pb and ^{228}Ac in the samples, and that

of ^{238}U was determined from the average concentrations of the ^{214}Pb and ^{214}Bi decay products (Hamby and Tynybekov, 2000). Thus, an accurate radiological concentration of ^{232}Th and ^{238}U was determined, whereas a true measurement of ^{40}K concentration was made. The specific activity (in *Bq kg*$^{-1}$), A_{Ei}, of a nuclide *i* and for a peak at energy *E*, is given by:

$$A_{Ei} = \frac{N_{Ei}}{\varepsilon_E \times t \times \gamma_d \times M_s} \tag{1}$$

where N_{Ei} is the Net Peak Area of a peak at energy *E*, ε_E the detection efficiency at energy *E*, *t* the counting live-time, γ_d the gamma ray yield per disintegration of the specific nuclide for a transition at energy *E*, and M_s the mass in *kg* of the measured sample. If there is more than one peak in the energy range of analysis, then the peak activities are averaged and the result is the weighted average nuclide activity.

Radiological concentrations of ^{232}Th, ^{238}U and ^{40}K were then converted into total elemental concentrations of thorium, uranium and potassium, respectively, according to the following expression:

$$F_E = \frac{M_E \cdot C}{\lambda_E \cdot N_A \cdot f_{A,E}} \cdot \frac{1}{n} \sum_{i=1}^{n} A_i \tag{2}$$

where F_E is the fraction of element *E* in the sample, M_E is the atomic mass *(kg mol*$^{-1}$*)*, λ_E is the decay constant *(s*$^{-1}$*)* of the parent radioisotope, N_A is Avogadro's number (6.023×10^{23} *atoms mol*$^{-1}$), $f_{A,E}$ is the fractional atomic abundance of ^{232}Th, ^{238}U or ^{40}K in nature, *C* is a constant (with a value of *100* or *1,000,000*) that converts the ratio of the element's mass to soil mass into a percentage or *ppm*, and A_i is the measured radiological concentration of ^{40}K (n=1) or that of the selected daughter radionuclides in the decay series of ^{232}Th and ^{238}U (n=2). Total elemental concentrations are reported in

units of *parts per million* (*ppm*) for thorium and uranium, and of *percent* (*%*) for potassium.

2.4 Derivation of the absorbed dose rates and effective dose rates

If natural radioactive nuclides are uniformly distributed in the ground, dose rates at 1 *m* above the ground surface are calculated by the following formula (Kohshi et al., 2001):

$$\textbf{Dose rate } (nGy\ h^{-1}) = \textbf{Radiological concentration } (Bq\ kg^{-1}) \times \textbf{Conversion factor } (nGy\ h^{-1}\ per\ Bq\ kg^{-1}) \quad (3)$$

In order to calculate the exposure rates 1 *m* above ground level for distributed sources of gamma emitters in soil, conversion factors (absorbed dose rate in air per unit activity per unit of soil mass, $nGy\ h^{-1}\ per\ Bq\ kg^{-1}$) were extensively calculated during the last forty years by many researchers. In the present work, the considered dose rate conversion factors for the ^{232}Th and ^{238}U series, and for ^{40}K, used in all dose rate calculations are those determined by Saito et al. (1990) and used extensively for all similar calculations in the UNSCEAR 1993 Report. It should be pointed out here that, using this calculation, the dose rate for the ^{232}Th and ^{238}U series is the average of the respective radiological concentrations multiplied by the conversion factors corresponding to each series. The total dose rate for each of the measured samples is the sum of the dose rates contributed by both series of ^{232}Th and ^{238}U, and by ^{40}K.

The building materials act as sources of radiation and also as shields against outdoor radiation (UNSCEAR 1993 Report). In massive houses made of different building materials such as stone, bricks, concrete or granite, the factor that mainly affects the indoor absorbed dose is the activity concentrations of natural radionuclides in those materials, while radiation emitted by sources outdoors is efficiently absorbed by the

walls. Consequently, dose rates in air indoors will be elevated accordingly to the concentrations of natural radionuclides used in construction materials. In order to facilitate the calculation of dose rates in air from different combinations of the three radionuclides in building materials and by applying the appropriate conversion factors, an activity utilization index is constructed that is given by the following expression:

$$\left(\frac{C_{Th}}{A_{Th}} f_{Th} + \frac{C_U}{A_U} f_U + \frac{C_K}{A_K} f_K \right) w_m \qquad (4)$$

where C_{Th}, C_U and C_K are actual values of the activities per unit mass ($Bq\ kg^{-1}$) of ^{232}Th, ^{238}U, and ^{40}K in the building materials considered; f_{Th}, f_U and f_K are the fractional contributions to the total dose rate in air from the standard or typical concentrations of these radionuclides. In the NEA 1979 Report, typical activities per unit mass of ^{232}Th, ^{238}U, and ^{40}K in building materials A_{Th}, A_U and A_K are referred to be 50, 50 and 500 $Bq\ kg^{-1}$, respectively. The activity utilization index is, finally, weighted for the mass proportion of the building materials in a house by being multiplied by a factor w_m that represents the fractional usage of those materials in the dwelling with the characteristic activity. For full utilization of a typical masonry ($C_{Th} = C_U = 50\ Bq\ kg^{-1}$ and $C_K = 500\ Bq\ kg^{-1}$) the activity utilization index is unity by definition and is deemed to imply a dose rate of 80 $nGy\ h^{-1}$.

Finally, in order to estimate the annual effective doses, one has to take into account the conversion coefficient from absorbed dose in air to effective dose and the indoor occupancy factor. In the UNSCEAR recent reports (1988, 1993, 2000), the Committee used 0.7 $Sv\ Gy^{-1}$ for the conversion coefficient from absorbed dose in air to effective dose received by adults, and 0.8 for the indoor occupancy factor, implying that 20 % of

time is spent outdoors, on average, around world. The effective dose rate indoors, in units of *mSv per year*, is calculated by the following formula:

$$\textbf{Effective dose rate (mSv y}^{-1}\textbf{) = Dose rate (nGy h}^{-1}\textbf{)} \times \textbf{24 h} \times \textbf{365.25 d} \times \textbf{0.8 (occupancy factor)} \times \textbf{0.7 Sv Gy}^{-1}\textbf{ (conversion coefficient)} \times 10^{-6} \quad (5)$$

In Table 2, the results obtained for the activity utilization index and the total absorbed dose rate in air for various fractional masses of the twenty-eight "granite" samples considered in this paper, as well as the indoor effective dose assessment for a specific fractional mass for each sample are displayed.

3. Results and discussion

Activity concentrations of ^{232}Th ranged from 1 to 906 *Bq kg*$^{-1}$, of ^{238}U from 1 to 588 *Bq kg*$^{-1}$ and of ^{40}K from 50 to 1606 *Bq kg*$^{-1}$. From the 28 samples measured in this study, "Café Brown" appears to have the highest concentrations for all the elements investigated, reaching levels of 906 *Bq kg*$^{-1}$ for ^{232}Th, 588 *Bq kg*$^{-1}$ for ^{238}U, and 1606 *Bq kg*$^{-1}$ for ^{40}K. "Rosso Balmoral" and "New Imperial" exhibit the second and third highest concentration of ^{232}Th reaching 490 *Bq kg*$^{-1}$ and 273 *Bq kg*$^{-1}$, respectively, and of ^{238}U reaching 162 *Bq kg*$^{-1}$ and 285 *Bq kg*$^{-1}$, respectively, while "Upatuba" appears to have the second higher concentration of ^{40}K reaching 1581 *Bq kg*$^{-1}$. All measured samples except of two, named "Astudo" and "Nero Africa", have concentrations of potassium above the value of 1000 *Bq kg*$^{-1}$. In addition, 13 samples appear to have concentration of ^{232}Th higher than 100 *Bq kg*$^{-1}$, while only 6 samples exhibit concentration of ^{238}U that surpass the above limit. "Nero Africa" demonstrates the lowest concentrations for all the investigated elements, showing zero activity levels for ^{232}Th and ^{238}U, and levels of 50 *Bq kg*$^{-1}$ for ^{40}K. Analytical results for the activity

concentrations of ^{232}Th, ^{238}U and of ^{40}K determined for each of the measured samples are displayed in Table 1.

The calculated elemental concentrations of thorium, uranium and potassium are plotted in Fig. 2 for the twenty-eight samples. The highest elemental concentrations of thorium are exhibited by the samples “Café Brown” and “Rosso Balmoral”, with values that reach levels of 222 and 120 *ppm*, respectively. “Café Brown” and “New Imperial” appear to have the highest concentrations of uranium reaching levels of 48 and 23 *ppm*, respectively. In addition, “Café Brown” and “Upatuba” present the highest concentrations of potassium reaching 5.3 and 5.2 %, respectively. The lowest concentrations of thorium, uranium and potassium are exhibited by “Nero Africa” and “Upatuba”, by “Nero Africa” and “Verte Brazil” and by “Nero Africa” and “ Astudo”, respectively. As it seems, “Café Brown” and “Nero Africa” appear to have the highest and the lowest elemental concentrations, respectively, for all the elements investigated. For comparison, Chiozzi et al. (2002) have performed a series of investigations on different rock types at the Alps-Apennines transition, Italy, and found elemental concentrations being in the range of 0.3–16.7 *ppm*, 0.3–5.6 *ppm*, and 0.14–5.14 %, for thorium, uranium and potassium, respectively. In addition, potassium concentrations in a wide variety of rock types are estimated to range from approximately 0.1 to 3.5 % (Kohman and Saito, 1954).

To estimate the effect of using atypical materials such as granites or other natural tiling rocks, it is necessary to determine the fractional utilization by mass for each of the measured samples and identify the associated dose rate. The activity utilization index estimated using the fractional contribution to the dose rate from the three radionuclides for the 28 samples are displayed in Table 2. As the mass fractional utilization of each radionuclide varies from sample to sample, the activity utilization index ranges from

0.09 for sample “Nero Africa” to 15.11 for sample “Café Brown”. It should be noted that, twenty-two of the measured samples appear to have an activity utilization index that ranges from 1.0 to 3.0, four of them surpass the above-mentioned range and only two samples have values under that range (≤ 1.0).

The total absorbed dose rates calculated from the concentrations of the nuclides of the ^{232}Th and ^{238}U series, and of ^{40}K, for full utilization of the measured tiling materials range from 7 to 1209 *nGy* h^{-1}, values that are decreased according to the fractional utilization of the materials. In round terms and for full utilization, 23 of the samples exhibit dose rates that range from 100 to 400 *nGy* h^{-1}, two exhibit dose rates under the typical limit of 100 *nGy* h^{-1} (“Nero Africa” with 7 *nGy* h^{-1} and “Astudo” with 43 *nGy* h^{-1}) and only three of the samples exhibit values over the limit of 400 *nGy* h^{-1} (“Café Brown” with 1209 *nGy* h^{-1}, “Rosso Balmoral” with 619 *nGy* h^{-1} and “New Imperial” with 409 *nGy* h^{-1}). A summary of this analysis is presented in Fig. 3, where the frequency (in *percent*) of total absorbed dose rates for full utilization of the twenty-eight measured samples is plotted.

The analytical results for the total absorbed dose rates in air for each of the measured samples and for various fractional masses indicated are also given in Table 2. For comparison, measurements in former Czechoslovakia, in houses with outside walls containing uraniferous coal slag, gave values approaching 1,000 *nGy* h^{-1} (Thomas et al., 1993), while measurements in a granite region of the United Kingdom, where some of the houses are made of local stone, gave 100 *nGy* h^{-1} (Wrixon et al., 1988).

The relative contribution to total absorbed dose due to ^{232}Th ranges from 1 % for sample “Nero Africa” to 69 % for “Rosso Balmoral”, due to ^{238}U ranges from 4 % for “Multi-colour” to 30 % for “Café Brown” and due to ^{40}K ranges from 7 % for “Café Brown” to

92 % for “Nero Africa”. The fractional contribution to total absorbed dose of the three radionuclides, ^{232}Th, ^{238}U and ^{40}K, is plotted in Fig. 4, for all the samples studied.

Finally, the annual effective doses indoors estimated, using a value of 0.7 $Sv\,Gy^{-1}$ for the conversion coefficient from absorbed dose in air to effective dose received by adults, 0.8 for the indoor occupancy factor and 0.5 utilization of material, range from 0.02 $mSv\,y^{-1}$ for sample “Nero Africa” to 2.97 $mSv\,y^{-1}$ for “Café Brown”. It is clear that, for full utilization of the materials, the associated effective dose rates would be by a factor of two higher than those illustrated in Table 2 ($w_m = 0.5$) and by a factor of two lower for one quarter utilization of the samples. However, the simple irradiation geometry and rounded values considered do not allow this approach to be more than a rough approximation.

4. Conclusions

Exploitation of high-resolution γ–ray spectroscopy provides a sensitive experimental tool in studying natural radioactivity and determining elemental concentrations and dose rates in various rock types. Most of the tiling rock samples studied in this work reveal high values for the activity and elemental concentrations of thorium, uranium and potassium, thus contributing to high absorbed dose rates in air. In general, the extracted values are distinctly higher than the corresponding population-weighted (world-averaged) ones, and, in some cases (e.g. “Café Brown”, “Rosso Balmoral”, “New Imperial” etc.), they lie outside the typical range variability of reported values from world-wide areas due to terrestrial gamma radiation, given in the recent UNSCEAR 2000 Report.

Acknowledgements

This work is conducted with financial support from the Cyprus Research Promotion Foundation (Grant No. 45/2001). We would also like to thank the Cyprus Association of Manufacturers, which provided us with the original granite materials from which the samples are prepared and gave us information about their origin.

References

Chiozzi, P., Pasquale, V., Verdoya, M., 2002. *Naturally occurring radioactivity at the Alps-Apennines transition.* Radiation Measurements 35, 147-154.

Florou, H., Kritidis, P., 1992. *Gamma radiation measurements and dose rate in the costal areas of a volcanic island, Aegean Sea, Greece*. Radiation Protection Dosimetry 45 (1/4), 277-279.

Hamby, D. M., Tynybekov, A. K., 2002. *Uranium, thorium and potassium in soils along the shore of lake Issyk-Kyol in the Kyrghyz Republic*. Environmental Monitoring and Assessment 73, 101-108.

Kohman, T., Saito, N., 1954. *Radioactivity in geology and cosmology*. Annual Review of Nuclear Science 4.

Kohshi, C., Takao, I., Hideo, S., 2001. *Terrestrial gamma radiation in Koshi prefecture, Japan*. Journal of Health Science, 47(4), 362-372.

Myrick, T. E., Berven, B. A., Haywood, F. F., 1983. *Determination of concentrations of selected radionuclides in surface soil in the U.S.* Health Physics 45(3), 631-642.

Nuclear Energy Agency (NEA), 1979. *Exposure to radiation from the natural radioactivity in building materials*. Report by NEA Group of Experts, OECD, Paris.

Saito, K., Petoussi, N., Zanki, M. et al., 1990. *Calculation of organ doses from environmental gamma rays using human phantoms and Monte Carlo methods*. Part 1, Monoenergetic sources of natural radionuclides in the ground, GSF-B2/90.

Snelling, A., Woodmorappe, J., 1998. *Rapid Rocks – Granites… they didn't need millions of years of cooling*. Creation Ex Nihilo 21(1), 37-39.

Thomas, J., Hulka, J., Salava, J., (1993). *New houses with high radiation exposure levels*. Proceedings of the International Conference on High Levels of Natural Radiation, Ramsar, 1990, IAEA, Vienna.

UNSCEAR, 1993. *Sources and Effects of Ionizing Radiation*. Report to General Assembly, with Scientific Annexes, United Nations, New York.

UNSCEAR, 2000. *Sources and Effects of Ionizing Radiation*. Report to General Assembly, with Scientific Annexes, United Nations, New York.

Wrixon, A. D., Green, B. M. R., Lomas, P. R. et al., 1988. *Natural radiation exposure in UK dwellings*. NRPB-R190.

TABLE CAPTIONS

Table 1. Samples nomenclature and origin; natural radioactivity concentrations of ^{232}Th, ^{238}U and ^{40}K in the measured samples. The small contribution of the environmental γ–ray background at the laboratory site has been subtracted from the spectra of the measured samples.

	Commercial name	Country of origin	Concentration ± Statist. Error (*Bq kg^{-1}*)		
			^{232}Th	^{238}U	^{40}K
1	Bianco Perla	Italy	37 ± 2	57 ± 2	1228 ± 48
2	Santa Cecilia	Brazil	85 ± 2	45 ± 1	1435 ± 55
3	Blue Paradise	Brazil	92 ± 3	15 ± 1	1246 ± 48
4	Blue Pearl	Belgium	77 ± 2	68 ± 2	1129 ± 44
5	Verte Brazil	Brazil	121 ± 3	5 ± 1	1200 ± 47
6	Upatuba	Africa	21 ± 1	17 ± 1	1581 ± 61
7	Verte Eukaliptos	Brazil	26 ± 1	45 ± 1	1522 ± 59
8	Red Africa	Africa	113 ± 2	57 ± 1	1360 ± 38
9	Tropical Japorana	Brazil	17 ± 1	13 ± 1	1048 ± 30
10	Astudo	Africa	32 ± 1	18 ± 1	254 ± 11
11	Baltic Brown	Brazil	136 ± 4	102 ± 3	1520 ± 58
12	Rosso Balmoral	Holland	490 ± 13	162 ± 5	1540 ± 60
13	Rossa Porino	Italy	172 ± 5	103 ± 3	1424 ± 55
14	Giallo Penere	Brazil	82 ± 2	31 ± 1	1230 ± 47
15	Nero Africa	Africa	0 ± 1	1 ± 1	50 ± 3
16	Rosa Beta	Italy	69 ± 2	40 ± 1	1124 ± 44
17	White Arabesco	N/A	146 ± 4	108 ± 3	1359 ± 52
18	Saint Tropez	Brazil	40 ± 1	8 ± 1	1021 ± 40
19	Kinawa	Brazil	101 ± 3	58 ± 2	1168 ± 45
20	Multi-colour	N/A	82 ± 2	10 ± 1	1486 ± 57
21	Capao Bonito	Brazil	190 ± 5	84 ± 2	1313 ± 51
22	New Imperial	N/A	273 ± 7	285 ± 8	1273 ± 49
23	Juparana	Brazil	265 ± 7	35 ± 1	1446 ± 56
24	Grand Paradisso	N/A	51 ± 1	29 ± 1	1013 ± 39
25	Café Brown	Brazil	906 ± 24	588 ± 16	1606 ± 62
26	Rosa Ghiandone	Italy	89 ± 3	57 ± 2	1047 ± 41
27	Jacaranda	Brazil	147 ± 4	68 ± 2	1031 ± 40
28	Colibri	Brazil	155 ± 4	53 ± 1	1365 ± 53

Table 2. The calculated activity utilization index and the total absorbed dose rate in air for various fractional masses of the measured samples, as well as the indoor effective dose assessment for a specific fractional mass for each sample.

Sample number	Activity utilization index	Absorbed dose rate* in air for indicated fractional mass of building material ($nGy\ h^{-1}$)				Effective dose rate indoors ($mSv\ y^{-1}$)
		$w_m = 1.0$	0.75	0.5	0.25	$w_m = 0.5$
1	1.72	137	103	69	34	0.34
2	2.09	168	126	84	42	0.41
3	2.03	163	122	81	41	0.40
4	1.76	141	106	70	35	0.35
5	2.38	190	143	95	48	0.47
6	2.49	199	149	100	50	0.49
7	2.19	175	132	88	44	0.43
8	2.23	179	134	89	45	0.44
9	1.61	129	97	64	32	0.32
10	0.54	43	32	22	11	0.11
11	2.66	213	160	106	53	0.52
12	7.73	619	464	309	155	1.52
13	2.96	237	178	119	59	0.58
14	1.87	150	112	75	37	0.37
15	0.09	7	6	4	2	0.02
16	1.65	132	99	66	33	0.32
17	2.67	214	160	107	53	0.52
18	1.51	121	91	60	30	0.30
19	1.96	157	118	78	39	0.38
20	2.28	183	137	91	46	0.45
21	3.11	249	187	124	62	0.61
22	5.11	409	307	205	102	1.00
23	4.39	351	263	176	88	0.86
24	1.44	115	86	57	29	0.28
25	15.11	1209	907	605	302	2.97
26	1.75	140	105	70	35	0.34
27	2.41	193	145	97	48	0.47
28	2.70	216	162	108	54	0.53

* **Conversion factors (K. Saito et al., 1990; UNSCEAR 1993 Report) in $nGy\ h^{-1}$ per $Bq\ kg^{-1}$: 0.623 for ^{232}Th series, 0.461 for ^{238}U series and 0.0414 for ^{40}K.**

FIGURE CAPTIONS

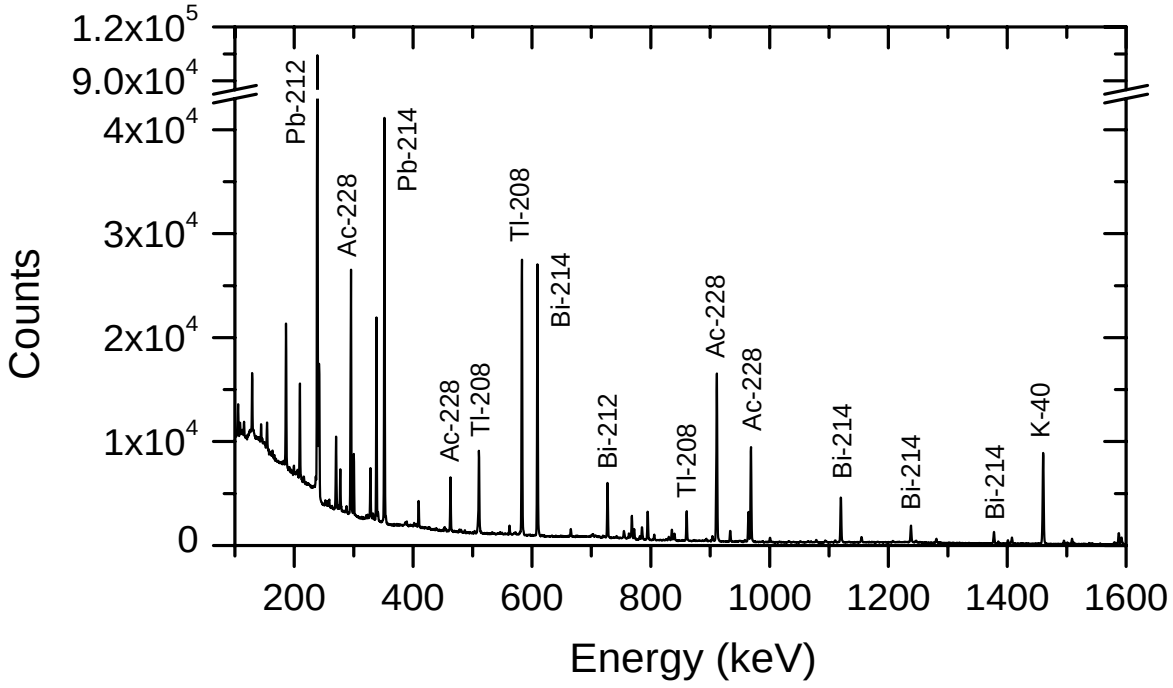

Figure 1. The interesting part of a typical γ–ray spectrum measured for sample 11 ("Baltic Brown"). The counting live-time was 37,000 *s e c* The important identified photopeaks and their associated radionuclides are depicted.

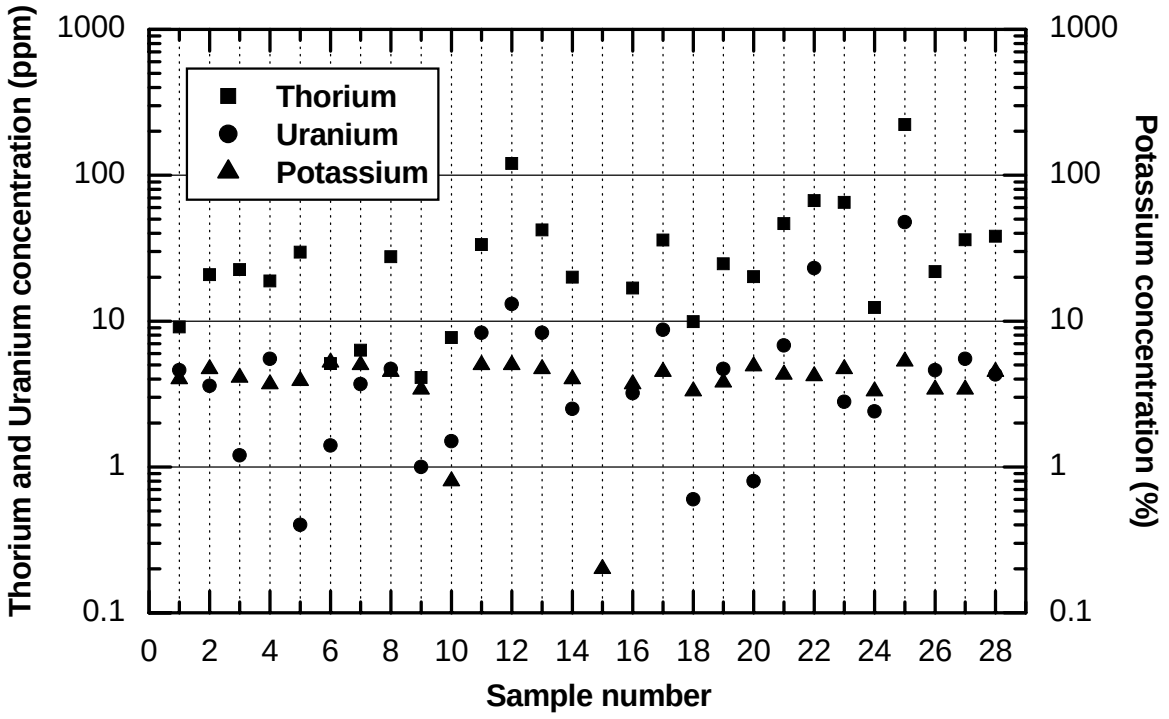

Figure 2. Thorium, uranium and potassium elemental concentrations in the samples of "granite" rocks imported in Cyprus. The sample numbers correspond to the sample description given in Table 1.

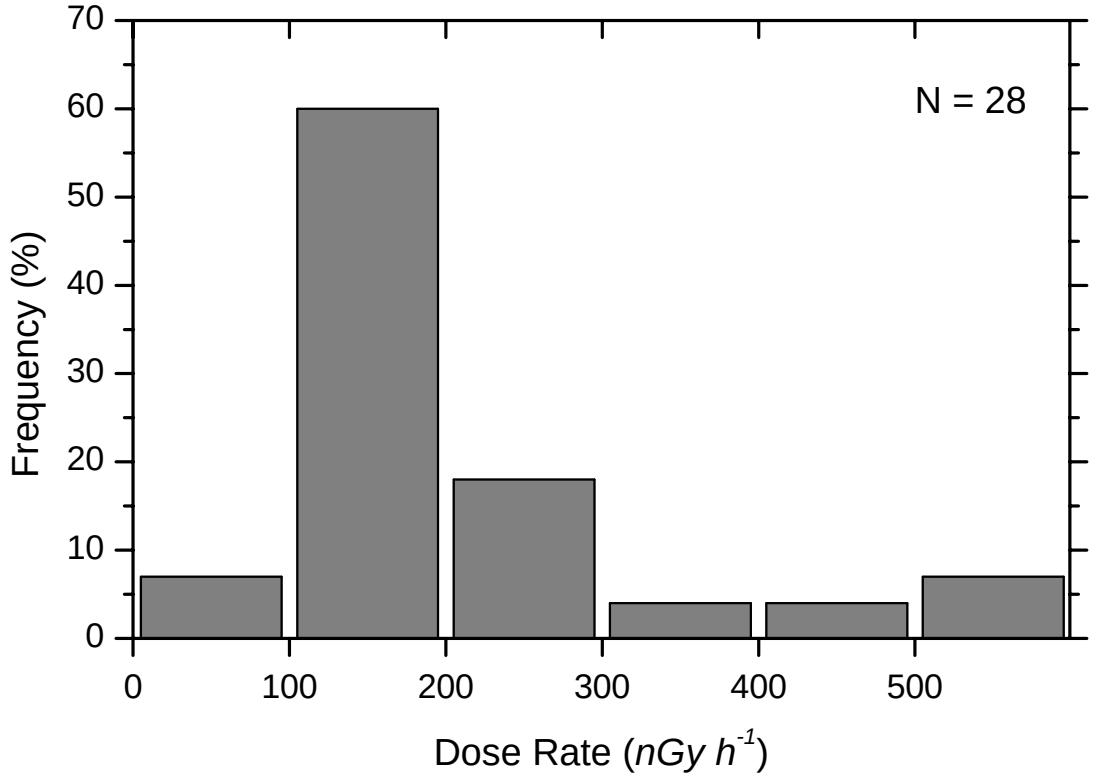

Figure 3. Frequency distribution of the total absorbed dose rates for full utilization of the twenty-eight measured "granite" samples. Last column represents those samples, which exhibit dose rates between 500 and 1300 $nGy\ h^{-1}$.

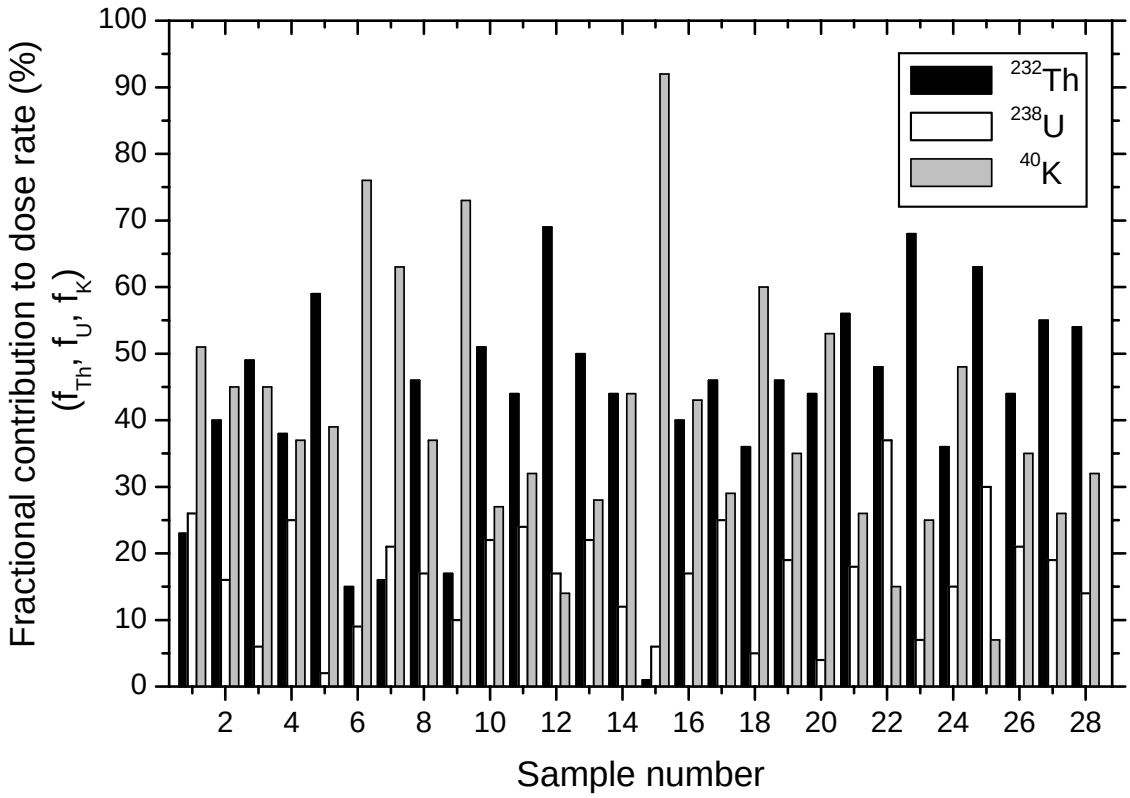

Figure 4. Thorium (^{232}Th) and uranium (^{238}U) decay series and potassium (^{40}K) percentage contribution to total absorbed dose rate in air for the measured samples. The sample numbers correspond to the sample description given in Table 1.